CILAMCE 2017
Florianópolis - Santa Catarina - Brazil

INFLUENCE OF INFILL-WALL MODELING IN THE BEHAVIOR OF REINFORCED CONCRETE FRAMES

Alessandro Onofre Rigão

rigaoa@gmail.com

Federal University of Santa Maria – Cachoeira do Sul Campus

Academic Center, Cachoeira do Sul, RS, Brazil.

Carlos Eduardo de Souza

João Kaminski Junior

carlos.souza@ufsm.br

jkj@ufsm.br

Federal University of Santa Maria – Technology Center

Technology Center, Santa Maria, RS, Brazil.

Abstract. *The influence of the infill-wall on the lateral stiffness of buildings has been the subject of studies since the 1950s. One of the most accepted methods in the academic environment, easy to implement computationally, to simulate the contribution of the panels is the substitution by an equivalent diagonal modeled as a jointed bar. However, this method is not able to represent adequately the change in straining in the boundary elements caused by the infill panels. Besides that, there is a dispersion of results when compared with more realistic methods in some cases. The use of structural model with more than one equivalent diagonal has shown more converging data for displacements and these are able to indicate better the stress-change in the frame boundary elements. The proposal of this work is to verify, through numerical simulation using a beam finite element, the change of the displacements and stresses in a reinforced concrete frame. Two models of equivalent diagonal are employed, namely Model A and Model B, but with use of two and three bars, adapted from literature proposals. These data are compared with simulation figures performed with micro-modeling using plane-stress finite elements.*

Keywords: *Infill-wall, Equivalent diagonal, Masonry, Finite element*

1 INTRODUCTION

It is a consensus in the technical means that infill-walls have the ability of absorbing and transmitting loading in buildings, altering the global behavior of the structure under effect of lateral loads. The evaluation of the masonry influence of the building stiffness has been subject of studies since the 1950 decade.

Among the first works on the subject, the work of Polyacov (1956) introduced the concept of equivalent diagonal bar substituting the infill panel. Based on that concept, other researchers studied and proposed similar formulations, like Holmes (1961), Stafford-Smith (1962), Mainstone (1962), Liauw and Kwan (1984), Moreira (2002), among others.

The basic premise of the equivalent diagonal, proposed by most studies about the contribution of infill panels in the stiffness of building frames, is the substitution of the panel by a diagonal pin-jointed strut (Fig. 1). The diagonal thickness usually is the same as the panels, but the width (W) is computed as a function of geometric and mechanical parameters of the wall and contour frame.

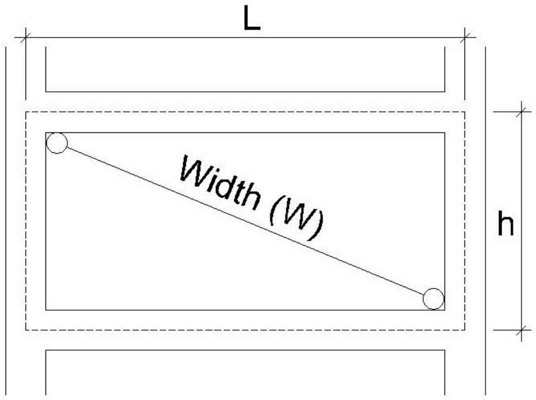

Figure 1. Equivalent diagonal model

The substitution of the infill panel by a diagonal bar shows to be advantageous, because of the low computational cost for its processing, simulating approximately the global behavior of the structure.

However, the various methods available in literature, when compared between each other or with more precise data, show disperse values for the displacements. Besides that, these models, normally, are not capable of capture the modification in shear and bending moment loads in the in the frame boundary elements caused by the infill wall.

The present work consists in assess the influence of the infill wall in the stiffness increase and in the loads on the boundary elements of a simple reinforced concrete frame by means of numerical simulation.

For that, it is intended to model the infill wall by a macro-model using the equivalent diagonal method, but adopting models that consider more than one bar as a strategy to better represent the panel contribution. Later on, the results will be compared to data obtained by Silva (2014).

Proceedings of the XXXVIII Iberian Latin-American Congress on Computational Methods in Engineering
P.O. Faria, R.H. Lopez, L.F.F. Miguel, W.J.S. Gomes, M. Noronha (Editores), ABMEC, Florianópolis, SC, Brazil, November 5-8, 2017.

The geometric and mechanic parameters of masonry and concrete frame will be the same as in Silva (2014). Among other analyses, they simulated reinforced concrete frames filled with ceramic masonry using the Finite Element Method (FEM) through a simplified micro-modeling with plane stress elements.

One of the models that substitute the infill wall by equivalent diagonal bars that will be tested is the model proposed by El-Dakhakhni et. al. (2003), which considered three equivalent diagonals. They considered a metallic frame and nonlinear analysis.

Other tested model considers two diagonals, as described in Fiore et. al. (2016), but with necessary modifications to consider reinforced concrete and linear material behavior, aiming to represent the same parameters as in Silva (2014). Fiore et. al. (2016) proposed the model aiming assessment of earthquake resistance.

Thus, in this work, the following conditions will be verified with diagonal elements and compared to the plane stress model of Silva (2014): (a) the lateral displacement at the top of the panel and (b) the normal and shear stress at a few points in the frame.

1.1 A short bibliography review

Silva (2014) studied infill wall frames fill with masonry filling in the Service Limit State (SLS). She considered the contribution of the panel in the frame stiffness by using the concept of well known equivalent diagonal, performing numerical analyses with the FEM with a simplified micro-modeling.

She adopted materials in the elastic phase, but considered problems of contact between the masonry and the frame by means of nonlinear analyses. She analyzed the maximum stress components (traction, compression, shear) in the elements and compared with the materials limit stress refering to cracking in relation to the SLS.

El-Dakhakhni et. al. (2003) performed nonlinear analyses to simulate the contribution of the masonry inserted in the metallic frame by means of three equivalent diagonal bars. These diagonals have their area shown in Fig. 2, being A the area of the infill wall.

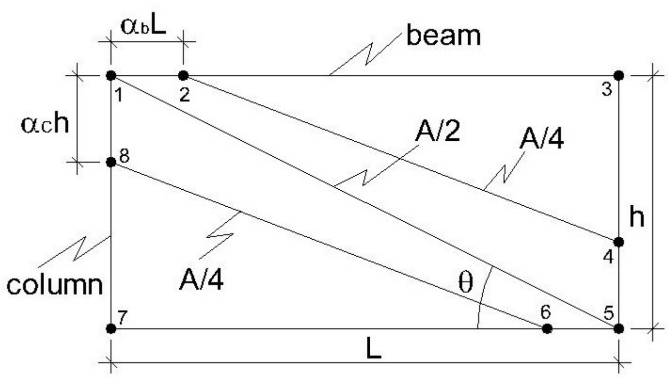

Figure 2. Model with three equivalent diagonal bars adopted by El-Dakhakhni et. al. (2003)

Fiore et. al. (2016) verified the contribution of the infill walls in the earthquake resistance, modeling them as two nonparallel diagonal with restraining points coinciding with the points where the resulting stress are applied on each side of the panel.

Proceedings of the XXXVIII Iberian Latin-American Congress on Computational Methods in Engineering
P.O. Faria, R.H. Lopez, L.F.F. Miguel, W.J.S. Gomes, M. Noronha (Editores), ABMEC, Florianópolis, SC, Brazil, November 5-8, 2017.

Results showed that with this methodology it is possible to capture the places with higher risks of failure by shear. In the work, two macro-models where used, one with a single diagonal and other with two, as shown in Fig. 3.

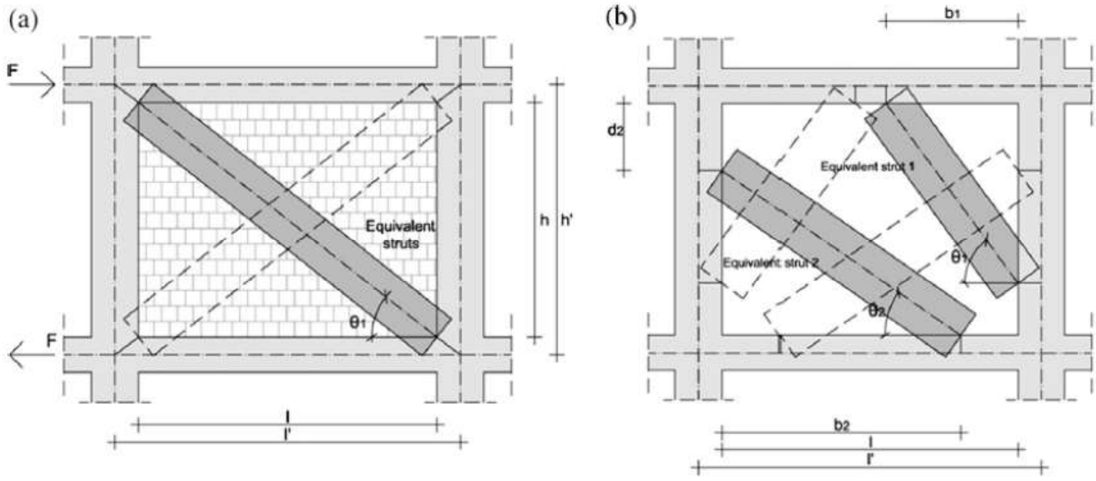

Figure 3. Models used by Fiore et. al. (2016)

Among their conclusions, the authors affirm that the double diagonal was efficient in capture critical points in which the shear stresses are above the limit given by the single diagonal or by the empty frame under earthquake loads.

A detailed simulation of the behavior of the masonry inserted in frames requires the knowledge of the structural behavior and various mechanical material parameters. Besides that, this kind of analysis demands and large coding and computational time.

Asteris (2008) developed a careful analysis of filled frames based on the complex behavior of panels under lateral loads. The basis of this study was done considering that the length and contact stress between the filling and the frame are estimated as part of the solution and was not assumed an "ad-hoc" analysis. He used this method to find the response of a simple frame of a floor under static load. The micro model used in that work discretize the wall in 3 elements: block as beam element, infill wall as plane element and interface as interface elements or unidirectional element connection.

Li et. al (2011) analyzed the contribution of the lateral resistance of the buildings non structural components (NSC). The performed numerical analyzes by FEM and compared with the main existing theoretical equations. The main goal was to quantify the stiffness gain of each component in a multi-floor building emphasizing the NSC.

Comparing the displacement and forces of the frame with infill wall analytically and by finite elements, it was verified that the analytical results presented lower displacements. Besides models that use only one bar, it is found in literature other models that use bar elements substituting the masonry.

Silva (2011), using the strut-and-tie model proposed by Alvarenga (2002), evaluated the structural behavior of steel plane frames filled with blocks of autoclaved aerated concrete. This model was later applied in the design of buildings with 4, 6 and 8 floors with steel bar bracings and masonry panels. The conclusions show that it is possible to substitute the metallic bracing bars by masonry panels until a certain number of floors. That depends on the frame stiffness, the masonry panels and the magnitude of the horizontal acting forces.

2 MODELS DESCRIPTION

The filled frame to be analyzes consists in a reinforced concrete frame with ceramic infill wall. The geometric dimensions are the same used in the typologies analyzed by Silva (2014), allowing results comparison.

The width of beams and columns are 19 centimeters, while the height of beams are 50 centimeters. For the columns height, different values were adopted: 40, 60, 80 and 100 centimeters. The frame dimensions are shown in Fig. 4.

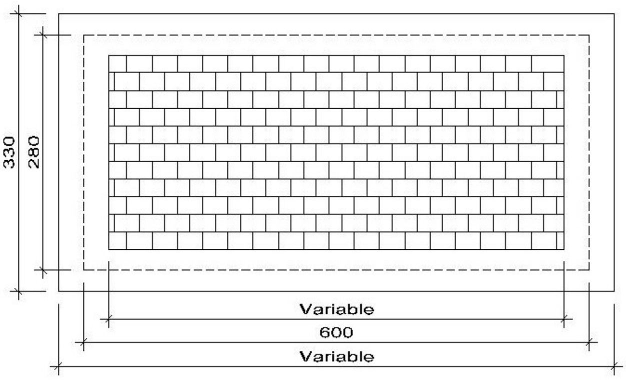

Figure 4. Filled frame dimensions (cm)

The dashed line represents the medium line that passes by the height of the structural elements, which are the dimension adopted for the finite element modeling.

All the models have the same theoretical height of h = 230 centimeters (useful height) and theoretical span L = 600 centimeters. The dimensions of the infill wall were modified (height x width) as function of the heights adopted for the columns (40, 60, 80 e 100 cm). Table 1 presents the dimensions of masonry infill walls for the analyzed frames as function of the columns height.

Table 1. Dimensions of masonry infill walls analyzed

Frame	Colum height (cm)	Masonry trickness (cm)	Masonry height (cm)	Masonry width (cm)
L_40	40	19	230	560
L_60	60	19	230	540
L_80	80	19	230	520
L_100	100	19	230	500

As mentioned before, the numerical modeling will be performed via finite elements, using the parameters proposed by the models of El-Dakhakhni et al. (2003) (called Model A) and Fiore et. al. (2016) (called Model B). However, these models are adapted to compare with values obtained by Silva (2014), through a linear elastic analysis.

The modeling of the infill wall will be performed using beam finite elements. The parts near to the connection between beam and columns will be considered as rigid, according to Brazilian standard NBR 6118:2014, which defines the length of these parts as function of the beams and columns height.

Extra nodes near the connecting nodes will be included to model these rigid sections. They are not shown in figures for clarity, since they are very close to the original connecting nodes. Table 2 presents the adopted geometric parameters of these rigid parts.

Table 2. Geometric parameters of rigid parts

Rigid part	Area (cm^2)	Inertia (cm^4)
Columns	11.400	342.000.000
Beams	5.320	34.757.333,33

It is considered that the infill wall does not bend, and thus the elements that simulate its contribution will have a large bending stiffness. This is done by considering a large inertia moment, equivalent to the relation of masonry thickness versus height, 19 cm x 230 cm, what leads to a value of 19.264.416,67 cm^4.

The masonry and reinforced concrete parameters are the same as in Silva (2014), which are summarized in Table 3.

Table 3. Mechanic parameters adopted for the materials

Material	Modulus of elasticity (MPa)	Poisson coefficient
Concrete	25.000	0,20
Masonry	900	0,15

2.1 Model A considerations

As shown in Fig 2., Dakhakhni et al. (2003) made use of three non parallel diagonal, where the total area A of the equivalent diagonal is expressed by:

$$A = \frac{(1-\alpha_C)\alpha_C ht}{\cos\theta} \tag{1}$$

Where α_C is the ratio of the panel's contact length in the column height, h is the useful frame height and t is the panel thickness.

The external diagonals are parallel between each other and their individual area represents 25 % of the total equivalent diagonal, while the central diagonal has 50 % of the total area.

The computation of α_b (ration of contact length of beam panel) and α_C, proposed in Dakhakhni et al. (2003), is function , among other factors, of the elements yielding moments, which must be lower than 0.4.

However, since the present work will focus on linear elastic analyses, there will be no yielding, and thus the adopted value for α_b and α will be 0.4, what is a value a little larger than suggested in bibliography (Holmes, 1961).

Making use of Eq.(1), the total area A of the equivalent diagonal is 1409 cm^2.

The external diagonal area is then 352,25 cm^2 and the central diagonal area is 704,5 cm^2. Also, the values of $\alpha_b L$ e $\alpha_C h$, obtained from the frame geometry, are 240 and 112 cm, respectively.

For the numerical implementation, the inertia moment is the same of model B for each diagonal, considering the width and total height of masonry (19 x 230 cm). The adopted proportion was the same for the areas division (25%, 50% and 25%).

This way, the external diagonals have inertia equal to 4.816.104,17 cm^4 and the central one, 9.632.208,33 cm^4.

The computed geometric parameters for beams and columns of model A are summarized in Table 4.

Table 4. Geometric parameters for beams and columns of model A

Frame	Beams inertia (cm^4)	Beams Area (cm^2)	Columns inertia (cm^4)	Columns area (cm^2)
L_40	197.916,67	950	101.333,33	760
L_60	197.916,67	950	342.000	1.140
L_80	197.916,67	950	810.666,67	1.520
L_100	197.916,67	950	1.583.333,33	1.900

2.2 Model B considerations

The proposal of this model is adapted from Fiore et. al. (2016), and the main characteristic is the use of non parallel diagonals, seen in Fig. (5). The position of the diagonals ends is defined as function of the panel dimensions.

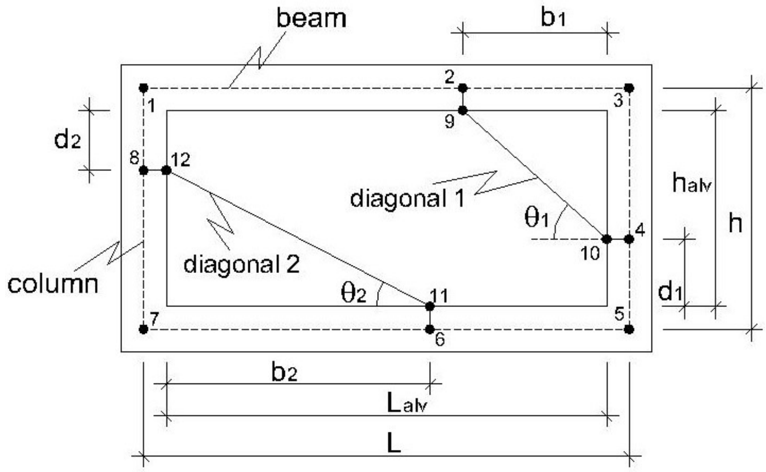

Figure 5. Model with two diagonal adapted from Fiore et. al. (2016)

For the case of a floor frame analysis, the following equations define those positions:

$$\frac{d_1}{h_{alv}} = 0{,}10834\left(\frac{L_{alv}}{h_{alv}}\right)^{-1} + 0{,}0073141\left(\frac{L_{alv}}{h_{alv}}\right)^{2} \tag{2}$$

$$\frac{b_1}{L_{alv}} = 0{,}48689\left(\frac{L_{alv}}{h_{alv}}\right)^{-2} + 0{,}16302\left(\frac{L_{alv}}{h_{alv}}\right)^{0,5} \tag{3}$$

$$\frac{d_2}{h_{alv}} = 0{,}157621\left(\frac{L_{alv}}{h_{alv}}\right)^{-1} + 0{,}084484\left(\frac{L_{alv}}{h_{alv}}\right)^{0,5} \tag{4}$$

$$\frac{b_2}{L_{alv}} = 0{,}408621\left(\frac{L_{alv}}{h_{alv}}\right)^{-0,5} + 0{,}44431\left(\frac{L_{alv}}{h_{alv}}\right)^{0,5} \tag{5}$$

Table 5 presents the resulting values for the above mentioned diagonals positions.

The area of the equivalent diagonal is obtained by the product wall thickness (t) by equivalent diagonal width (w). In this models, the area is divided equally for both diagonals.

Table 5. Diagonal position in frames

Frame	d_1 (cm)	b_1 (cm)	d_2 (cm)	b_2 (cm)
L_40	20,21	188,44	45,21	534,89
L_60	19,89	182,58	45,21	280
L_80	19,62	176,99	45,25	488,71
L_100	19,41	171,69	45,33	466,12

There are many formulations in literature (Mainstone & Weeks, 1970; Liauw & Kwan, 1984; Durrani & Luo, 1994; Chrysostomou & Asteris, 2012) for the calculation of the equivalent width, which depend of the frame geometry and masonry mechanical properties and contour elements.

It was adopted the formulation proposed by Mainstone and Weeks (1970), given by the following equation:

$$w = 0{,}175(\lambda_H)^{-0{,}4}.D \quad (6)$$

Where λ_H is the product between the relative stiffness λ and the height of free spam beam, and D is the length of the equivalent diagonal.

This equation was employed by Silva (2014), and results close to the finite element model were obtained.

The relative stiffness λ is computed as:

$$\lambda = \sqrt[4]{\frac{E.t.sen(2\theta)}{4.E_P.I_P.h}} \quad (7)$$

Where E is the masonry elastic modulus, t is the masonry thickness, θ is the diagonal angle, E_p is the column elastic modulus, I_p is the column inertia moment and h is the masonry height.

It is verified, in this model, that the equivalent diagonal bars do not connect directly with the beams and columns medium line. Because of that, new nodes where inserted to allow their connection.

The properties of these bars are the same as of the beams and columns to which they connect, with 3 degrees of freedom, considering as rigid elements with inertia and area equivalent to the thickness and length of these parts.

The geometric parameters of the transversal section for beams and columns are the same of model A.

Table 6 presents the geometric properties computed for these rigid parts of beams, columns and masonry diagonals.

Table 6. Geometric properties for rigid parts and diagonals

Frame	Inertia rigid parts (cm^4)	Area rigid parts (cm^2)	Area diagonals (cm^2)	Inertia diagonals (cm^4)
Beams	342.000.000	11.400	-	-
L_40	19.264.416,67	4.370	770,67	9.632.208,33
L_60	19.264.416,67	4.370	841,68	9.632.208,33
L_80	19.264.416,67	4.370	886,57	9.632.208,33
L_100	19.264.416,67	4.370	915,18	9.632.208,33

The areas of the diagonals transversal section are considered as half of the value obtained by the propostal of Mainstone e Weeks (1970). The same applies to the value of the inertia moment, what was adopted as 50 % of the wall total inertia moment, in order to make it very stiff for bending.

For comparison between models A and B, the nodal constraints occur at nodes 5 (directions x and y) and 7 (direction y). It was considered the direction x as horizontal and y as vertical.

An horizontal force is applied on node 1, at the top of the frame, in both models. The force magnitudes are the same as in Silva (2014).

Table 7 presents the values of the horizontal forces applied at different frames as function of the columns heights.

Table 7. Force applied on frames

Frame	Horizontal force (kN)
L_40	62,48
L_60	93,10
L_80	113,49
L_100	131,52

2.3 Description of finite element formulation

The numerical simulations were performed using the beam finite element. The element contains 3 degrees of freedom per node, two translations and one rotation.

The element formulation might be obtained by the minimization of the total potential energy functional Π = U - W, where U is the deformation energy and W the work done on the system.

The function for the potential energy over an area Ω without body forces is given by:

$$\Pi_{\mathrm{p}} = \frac{1}{2}\int_{\Omega} \boldsymbol{\sigma\varepsilon}\mathrm{d}\Omega - \int_{\Omega} \mathbf{p}(\mathbf{s})\mathbf{u}(\mathbf{s})\mathrm{d}\Omega \tag{8}$$

Where $\boldsymbol{\sigma}$ and $\boldsymbol{\varepsilon}$ are the infinitesimal stress and deformation tensors.

As a form of facilitating the deduction of element matrices, the element can be decomposed in bar and beam components.

For the bar, the axial displacements are considered, and for the beam, the transversal and rotation are considered.

The detailed deduction of such element can be found in many classical references, such as Hinton and Owen (1980), and will not be repeated here.

The resulting equations form a linear system composed by the global stiffness matrix that is assembled as a superposition of the element stiffness matrix.

The element matrix contains 3 degrees of freedom, and is given by:

$$\mathbf{K_e} = \begin{bmatrix} \frac{\mathrm{EA}}{\mathrm{L}} & 0 & 0 & -\frac{\mathrm{EA}}{\mathrm{L}} & 0 & 0 \\ 0 & \frac{12\mathrm{EI}}{\mathrm{L}^3} & \frac{6\mathrm{EI}}{\mathrm{L}^2} & 0 & -\frac{12\mathrm{EI}}{\mathrm{L}^3} & \frac{6\mathrm{EI}}{\mathrm{L}^2} \\ 0 & \frac{6\mathrm{EI}}{\mathrm{L}^2} & \frac{4\mathrm{EI}}{\mathrm{L}} & 0 & -\frac{6\mathrm{EI}}{\mathrm{L}^2} & \frac{2\mathrm{EI}}{\mathrm{L}} \\ -\frac{\mathrm{EA}}{\mathrm{L}} & 0 & 0 & \frac{\mathrm{EA}}{\mathrm{L}} & 0 & 0 \\ 0 & -\frac{12\mathrm{EI}}{\mathrm{L}^3} & -\frac{6\mathrm{EI}}{\mathrm{L}^2} & 0 & \frac{12\mathrm{EI}}{\mathrm{L}^3} & -\frac{6\mathrm{EI}}{\mathrm{L}^2} \\ 0 & \frac{6\mathrm{EI}}{\mathrm{L}^2} & \frac{2\mathrm{EI}}{\mathrm{L}} & 0 & -\frac{6\mathrm{EI}}{\mathrm{L}^2} & \frac{4\mathrm{EI}}{\mathrm{L}} \end{bmatrix} \tag{9}$$

Where E is the material elastic modulus, A and I are the transversal section area and inertia moment and L is the element length.

In this study, it was considered that the elements referring to the masonry did no transmit moments to the contour structural elements, and thus, their nodes were considered as pinned. This way, these elements have only the axial stiffness terms EA/L, and the other elements are zero.

The transformation of the stiffness matrix from Eq. (20), what is writen in the element coordinates, into the global coordinate system, is performed via se following transformation:

$$\mathbf{K_{gl}} = \mathbf{T^T}.\mathbf{K_e}.\mathbf{T} \tag{10}$$

Where the rotation matrix given by:

$$\mathbf{T} = \begin{bmatrix} \cos\alpha & \sin\alpha & 0 & 0 & 0 & 0 \\ -\sin\alpha & \cos\alpha & 0 & 0 & 0 & 0 \\ 0 & 0 & 1 & 0 & 0 & 0 \\ 0 & 0 & 0 & \cos\alpha & \sin\alpha & 0 \\ 0 & 0 & 0 & -\sin\alpha & \cos\alpha & 0 \\ 0 & 0 & 0 & 0 & 0 & 1 \end{bmatrix} \tag{11}$$

For post processing the displacement equilibrium analysis, a vector with displacements at each element and the element stiffness matrix are assembled, what allow computation of internal forces in global coordinates. The coordinate transformation matrix is employed to obtain the forces in the element coordinate system, and then compute resulting stress components.

Once the normal and tangential forces and the bending moments are available, the normal stress at the top and bottom of the cross section and the shear stress are computed in the following way:

$$\sigma_{\mathrm{Top}} = \frac{\mathrm{N}}{\mathrm{A_e}} - \frac{\mathrm{M.c}}{\mathrm{I}} \tag{12}$$

$$\sigma_{\mathrm{Bot}} = \frac{\mathrm{N}}{\mathrm{A_e}} + \frac{\mathrm{M.c}}{\mathrm{I}} \tag{13}$$

$$\tau_{\mathrm{Med}} = \frac{\mathrm{V.f}_f}{\mathrm{A_e}} \tag{14}$$

Where σ_{Top} and σ_{Bot} are the normal stress at top and bottom, respectively, τ_{Med} is the average shear stress, N and V are the normal and the tangential force on the element, f_f is the shape factor (adopted here as 1,0), M is the bending moment, $\mathrm{A_e}$ and I are the cross section area and inertia, and c is the distance between the neutral line to the point of stress computation in the cross section.

3 RESULTS AND DISCUSSION

The comparison between maximum displacements of the analysed models in relation to results obtained by Silva (2014) were performed through the verification of the maximum horizontal displacement at the top of frames on node 3 of both models.

Table 8 presents the horizontal displacements found in the simulations and Fig. 9 compares the displacements between models and those of Silva (2014).

Table 8. Horizontal displacement found in the simulations

	Horizontal displacement (mm)			
	P40	P60	P80	P100
Model A	2,198	2,577	2,719	2,800
difference	*37,12%*	*30,68%*	*27,35%*	*30,11%*
Model B	1,766	2,159	2,287	2,339
difference	*10,17%*	*9,48%*	*7,12%*	*8,69%*

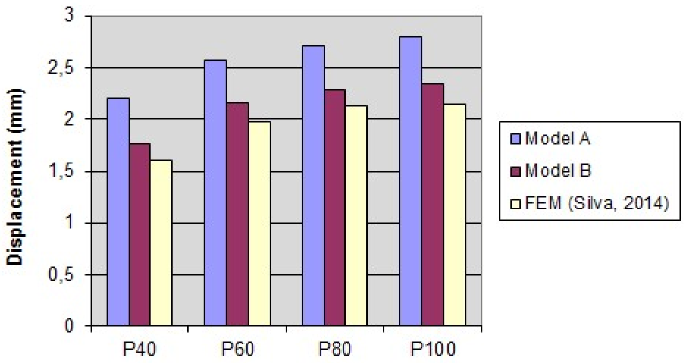

Figure 9. Displacements for models

Comparing the linear models results in relation to the plane model with simplified micromodeling, it is observed that the linear modes present larger displacements.

The differences were higher for model A, where the displacements were higher than 27%.

However, model B present displacements compatible to the simulation of Silva (2014), at order of 10 % difference, showing more trustful for the analyzes performed.

When comparing the structure of both analyzed models, it is seem that model B does not use of the central diagonal. Besides that, the connections of the masonry diagonals occur closer to the connection beam-columns when compared to model A, what should make it more flexible. Despite that, his model is stiffer than model A.

One possible reason for this behavior might be consideration of the masonry panel dimensions in the formulation of diagonals positioning in the frame.

Even then, it is suggested that both models can be used in calculation of displacements estimative in place of plane models, due to its higher simplicity and easier simulation. It is important to have in mind, though, that model A might present larger displacements.

Besides that, it is suggested to perform more comparisons between the displacements obtained for models A and B with experimental data in order to better validate the models for future works.

The comparative analysis between internal loads obtained by linear models in relation to the plane element was preformed through the reading of the normal tensile and compressive stress (σ_T e σ_C) and shear (τ_{xy}) from simulations of Silva (2014) along the transversal section of elements that showed to be more critical.

The reading was performed in two different positions on columns of frames P60, P80 and P100: at the top right extremity (node 3) and bottom right (node 5). These readings were compared with medium values at the same positions obtained by Silva (2014). The normal stress readings were taken at position farthest to the beam neutral line in the element cross section.

Frame stress was measured immediately before points 3 and 5 on the beams (before the rigid parts) so that the stress measuring point was the same for all frames, besides avoiding imprecise data due to the rigid parts.

Tables 9 and 10 present the stress obtained at those points and Fig. 10 and Fig. 11 show a comparison among data.

Table 9. Stress on top of frames in right side

		Frames stresses on node 3 (MPa)		
		P60	P80	P100
Model A	σ_T	4,284	5,473	6,449
	σ_C	-4,816	-6,19	-7,336
	τ_{xy}	0,124	0,167	0,206
Model B	σ_T	2,691	3,450	4,054
	σ_C	-3,103	-4,031	-4,795
	τ_{xy}	0,017	0,040	0,061
Silva (2014)	σ_T	2,744	3,221	2,805
	σ_C	-4,492	-3,844	-4,421
	τ_{xy}	0,784	0,619	0,769

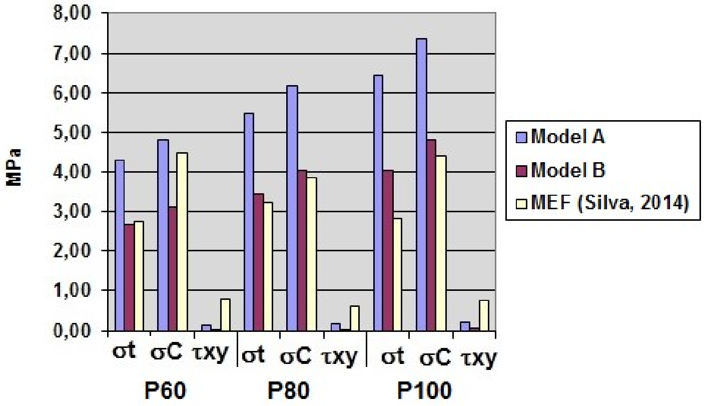

Figure 10. Stresses for models on node 3

Table 10. Stress on base of frames in right side

		Frames stresses on node 5 (MPa)		
		P60	P80	P100
Model A	σ_T	5,072	6,284	7,266
	σ_C	-5,834	-7,247	-8,411
	τ_{xy}	0,178	0,225	0,268
Model B	σ_T	3,122	4,189	5,073
	σ_C	-4,37	-5,677	-6,767
	τ_{xy}	0,267	0,327	0,38
Silva (2014)	σ_T	4,236	3,113	2,71
	σ_C	-5,093	-5,779	-6,278
	τ_{xy}	0,785	0,619	0,428

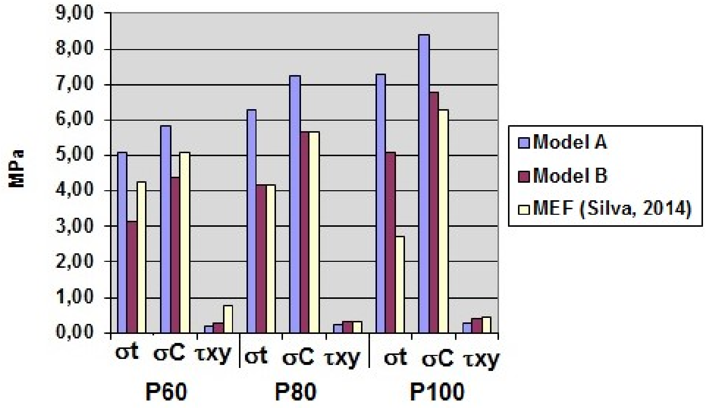

Figure 11. Stresses for models on node 5

When comparing data from linear models in relation to the plane model on node 3, it is observed that the normal stress components were superior in almost all cases. The exception occurred for compressive stress in model B for frame P60, where the obtained value was lower in relation to model of Silva (2014).

Comparing both models, the reading for normal stress of model B were closer to the plane model, while model A gave much higher values in all cases, showing not adequate for this kind of analysis.

When analyzing the shear stress components of linear models, it is verified that these presented values relatively lower than in the plane models. Model B presented the larger differences.

Analyzing the normal stress on node 5, it is observed a similar behavior to the observed on node 3. The normal stress were superior in almost all cases, with exception of frame P60 for model B, where the normal stress values were lower than in the reference model.

When performing a comparison between models, for a same stress measure, model A shows a tendency to higher stress in relation to model B, showing values more distant those obtained by Silva (2014).

At node 5, the shear stress also presented values lower than the plane model. However, these differences were smaller than in node 3. Again, the worst case happens for frame P60.

Because it was employed beam elements for the study of stress, errors are expected in the areas with larger stress concentration or in points with large variation in cross section, as in the case of chosen nodes. It is believed that this might be one of the reasons for the data dispersion.

When comparing the stress among the two linear models, it is observed that model A presents a tendency to present larger normal stresses.

In shear, model A showed larger values on node 3, and model B it happened on node 5.

Taking into consideration that the model of Silva (2014) presents values that can be considered as reference for stress, model B showed more adequate to estimate normal stresses, having in mind the limitations of these linear models.

Because of the stress analysis results dispersion, it is suggested a better study of the equivalent diagonals dispersion. Also, other proposals for the equivalent masonry diagonal width found in literature should be considered, aiming convergence of the stress in relation the plane models.

4 CONCLUDING REMARKS

It was performed the analysis of frames made of reinforced concrete with masonry infill walls using linear elastic beam finite elements. The masonry was substituted by equivalent diagonal elements and the displacements and stress components were evaluated. Two variations of the basic model were considered, one with two and other with three diagonals.

When comparing with values shown in reference Silva (2014), the analysis of displacements at the top of the frames presented values nearly 30% above for model A and of the order of 10% for model B. The differences were larger for frames with columns with lower dimensions. Having in mind the modeling simplicity, it is considered that it is viable to use model B for displacements estimation.

The analysis of normal stress at critical nodes showed that model B results are closer to the reference plane stress model. The shear stresses, however, were lower than the plane stress model.

REFERENCES

ABNT NBR 6118:2104. Projeto de estruturas de concreto-Procedimento. Rio de Janeiro.

Alvarenga, R. C. S. S., 2002. *Análise teórico-experimental de estruturas compostas de pórticos de aço preenchidos com alvenaria de concreto celular autoclavado*. thesis, University of São Paulo/São Carlos.

Asteris, P. G., 2008. Finite element micro-modeling of infilled frames. *Electronic Journal of Structural Engineering*, v.8, pp.1-11.

Chrysostomou, C. Z., Asteris, P. G., 2012. On the in-plane properties and capacities of infilled frames. *Engineering Structures*, v.41, Aug, pp.385-402.

Durrani, A. J., Luo, Y. H., 1994. Seismic retrofit of flat-slab buildings with masonry infills. *Proceedings from the NCEER Workshop on Seismic Response of Masonry Infills*, National Center for Engineering Earthquake, Buffalo, N.Y.

El-Dakhakhni, W. W., Elgaaly, M. & Hamid, A. A., 2003. Three-strut model for concrete masonry-infilled stell frames. *Structures Engineering ASCE*, v. 129, pp. 177-185.

Fiore, A., Spagnoletti, G., & Greco, R., 2016. On the prediction of shear brittle collapse mechanisms due to the infill-frame interaction in RC under pushover analysis. *Engineering Structures*, v. 121, pp. 147-159.

Hinton, E. & Owen, D. R. J., 1980. An Introduction to Finite Element Computations *Pineridge Press Ltd*.

Holmes, M., 1961. Steel Frames with Brickwork and Concrete Infilling. *Proc. Inst. Civ. Eng*, v. 19, pp. 473-478.

Li, B., Hutchinson, G. L. & Duffield, C. F., 2011. The influence of non-structural components on tall building stiffness. *Struct. Desing Tall Spec*., v.20, p.853-870, 2011.

Liauw, T.C., & Kwan, K.H., 1984. Nonlinear behavior of non-integral infilled frames. *Computers and Structures*, v.18, n.3, pp. 551-560.

Mainstone, R.J., Weeks, G. A., 1970. The influence of bounding frame on the racking stiffness and strength of bricks walls. Proceedings of the 2nd International Conference on Brick Mansory, *Building Research Establishment*, pp.165-171.

Mainstone, R. J., 1971. Supplementary Note on the Stiffness and Strength of Infilled Frames. CP13 74, *Build. Res. Establishment*. London, UK, v. 88, n. ST6, pp. 183-199.

Moreira, T. V., 2002. *Análise da sensibilidade dinâmica de edifícios com estruturas esbeltas*. thesis, Federal University of Rio de Janeiro/Rio de Janeiro.

Polyakov, S. V., 1956. Masonry in framed buildings. *National Lending Library for Science and Technology*, Boston.

Silva, L. R. da., 2014. *Modelagem de pórticos de concreto armado preenchidos com a consideração de aberturas nos painéis de alvenaria*. dissertation, Federal University of Santa Maria/Santa Maria.

Silva, R. L.,2011. *Avaliação de pórticos planos de aço considerando a contribuição da alvenaria pelo modelo de bielas e tirantes*. dissertation, Federal University of Viçosa/Viçosa.

Starfford-Smith, B., 1962. Lateral stiffness of infilled frames. *ASCE Journal of Structural Division*, v. 88, n. ST6, pp. 183-199.